International Journal of Greenhouse Gas Control 155 (2026) 104743

Contents lists available at ScienceDirect

International Journal of Greenhouse Gas Control

journal homepage: www.elsevier.com/locate/ijggc

Global strategic deployment of Direct Air Capture technologies

Kenneth Okosun [a,b,*], Henrik Wenzel [a,b], Freia Harzendorf [a], Thomas Schöb [a], Mak Đukan [a], Jochen Linßen [a], Detlef Stolten [b], Jann M. Weinand [a]

[a] Forschungszentrum Jülich GmbH, Institute of Climate and Energy Systems – Jülich Systems Analysis (ICE-2), 52425, Jülich, Germany

[b] RWTH Aachen University, Chair for Fuel Cells, Faculty of Mechanical Engineering, 52062, Aachen, Germany

ARTICLE INFO

Keywords:
Direct air capture
Techno-economic assessment
Weather-dependent performance
Geospatial analysis
Carbon dioxide removal
Renewable energy integration
Energy system modeling

ABSTRACT

Direct Air Capture (DAC) is a promising negative emission technology with the potential to remove excess CO_2 from the atmosphere. The levelized cost of solid sorbent (S-DAC) and liquid solvent DAC (L-DAC) is highly region-specific, driven by variability in weather conditions and renewable energy potential. This necessitates a holistic, global assessment that combines these two technologies with the highest technology readiness levels to identify cost-optimal locations for DAC deployment. Here, we identified optimal locations for S-DAC and L-DAC using an hourly cost optimization model that incorporates weather-driven performance and region-specific solar, wind, and geothermal energy resources under fully electric and hybrid energy configurations, where hybrid systems combine electric and direct renewable heat. We show that DAC deployment is cost-optimal in regions combining low renewable energy costs with favorable weather conditions, with S-DAC favored in Australia, Iceland, Mexico, and parts of Asia, and L-DAC in much of South America and Sub-Saharan Africa. The energy configuration strongly influences costs, with hybrid systems resulting in lower global levelized costs of DAC in 2050 ranging from 160 to 1720 €/tCO_2, with a median of 271 €/tCO_2. Our study further reveals that DAC can achieve a deployment level of 2 $GtCO_2$/a at costs below 195 €/tCO_2 in cost-optimal regions. At the same time, substantial uncertainty remains in future cost estimates, with global median values ranging from 144 to 392 €/tCO_2 depending on underlying techno-economic assumptions. These results emphasize the importance of holistic, region-specific assessment to guide strategic and cost-effective global DAC deployment, aligned with the cost-efficiency principles in Article 6 of the Paris Agreement.

1. Introduction

Global CO_2 emissions currently amount to approximately 37 $GtCO_2$ per year and are projected to rise to over 50 $GtCO_2$ by 2050 under the existing climate protection measures, even with continued deployment of renewable energy technologies (IPCC, 2022; Beuttler et al., 2019; Wei et al., 2025). Such emission trajectories are incompatible with limiting global warming to 1.5 – 2 °C, as outlined in the Paris Agreement. Achieving these targets will require both substantial emissions reductions through conventional mitigation measures, such as energy efficiency improvements, electrification, and fuel switching, and the large-scale deployment of carbon dioxide removal (CDR) to address residual and hard-to-abate emissions. Total CDR deployment is projected to reach approximately 6 – 10 $GtCO_2$ per year by 2050 (Smith et al., 2024). Among the available CDR options, Direct Air Capture and Storage (DACS), which involves capturing CO_2 directly from the ambient air and permanently storing it, is considered a promising pathway due to its scalability, relative ease of monitoring the amount of captured and stored CO_2, and long-term storage durability (Smith et al., 2024; Küng et al., 2023). Within this context, Direct Air Capture (DAC) refers specifically to the CO_2 capture step and represents the core technological component as well as the main cost driver of DACS, making it the primary focus of this study. DACS is expected to contribute approximately 0.5 – 5 $GtCO_2$ in 2050 (IPCC, 2022; IEA, 2022; Fuss et al., 2018). However, existing DAC plants have a combined operational capacity of around 40 $ktCO_2$ per year (Van Der Spek et al., 2025), highlighting the substantial scale-up required to realize this potential.

High levelized costs of CO_2 removal stemming from high energy consumption, substantial sorbent costs, and significant capital expenses are currently the main limiting factors for large-scale DAC deployment (Küng et al., 2023; IEA, 2022). These costs are highly sensitive to local weather conditions, as well as electricity and heating costs. Air

* Corresponding author.
E-mail addresses: k.okosun@fz-juelich.de (K. Okosun), m.dukan@fz-juelich.de (M. Đukan).

https://doi.org/10.1016/j.ijggc.2026.104743
Received 2 March 2026; Received in revised form 3 July 2026; Accepted 7 July 2026
Available online 17 July 2026

temperature and relative humidity influence DAC productivity as well as energy consumption, and, in the case of liquid solvent systems, water consumption, thereby influencing the levelized DAC cost (An et al., 2022; Sendi et al., 2022; Shorey and Abdulla, 2024; Terlouw et al., 2024). In turn, local renewable energy potentials, such as the availability of low-cost solar PV or geothermal heat, also play a crucial role in cost reduction, given the high energy consumption of DAC technologies (Krull et al., 2025). For instance, capturing 1 $GtCO_2$ using a fully electrified amine-functionalized solid sorbent process would consume 1450 – 2560 TWh_{el}, depending on the prevailing weather conditions (Sendi et al., 2024). This energy consumption represents 5.4 – 9.5% of the world's electricity consumption in 2023 (U.S. Energy Information Administration, 2025). Therefore, identifying locations where DAC can be deployed at the lowest cost – by combining favorable weather conditions with low-cost renewable energy sources – is essential for enabling cost-effective large-scale deployment.

In addition, cost-effective deployment requires selecting the DAC technology best suited to local weather conditions and available energy resources. At the moment, the two DAC technologies with the highest Technology Readiness Level are liquid solvent (L-DAC) and solid sorbent DAC (S-DAC) (IEA, 2025). L-DAC systems employing an aqueous alkali hydroxide solution in a calcium looping cycle for CO_2 capture maintain high capture efficiencies and lower energy requirements in hot, humid climates, but are prone to freezing at sub-zero conditions, potentially limiting operation to warmer regions or seasons (An et al., 2022; Shorey and Abdulla, 2024; Holmes and Keith, 2012; McQueen et al., 2021). By contrast, amine-functionalized S-DAC systems perform well in cold, moderately humid conditions where adsorption kinetics remain favorable and freezing risks are minimal (Sendi et al., 2022; Jajjawi et al., 2026). This climate-technology matching suggests that L-DAC may be more competitive in tropical regions while S-DAC holds advantages in colder climates, motivating our comparative geospatial cost assessment.

Existing studies have performed cost assessments for Mt- to Gt-scale DAC systems (Young et al., 2023; Sievert et al., 2024; IEAGHG, 2021; Keith et al., 2018). However, they have limited temporal and spatial coverage, ignoring the variability in weather conditions and renewable energy potential. Additionally, other studies focus on a single DAC technology, thereby eliminating the opportunity for DAC cost comparison across different regions (Terlouw et al., 2024; Sendi et al., 2024). Hence, a comprehensive global evaluation combining both technologies remains absent, with existing joint analyses restricted to single countries (Wenzel et al., 2025; Boerst et al., 2024). With L-DAC and S-DAC at the forefront of DAC development, it is crucial to evaluate how weather and renewable energy potential influence global DAC deployment, identifying cost-effective locations. Hence, the main research questions this study seeks to answer are: (1) *How do region-specific weather conditions and renewable potentials shape the spatial variation in the levelized cost of DAC?* and (2) *Which combination of regions offers the lowest-cost pathway to achieve a global gigaton-scale DAC capacity in 2050?*

Our study presents the first global comparison of L-DAC and S-DAC, providing insights into the strategic deployment of DAC in 2050 by prioritizing regions with suitable weather conditions and accessible low-carbon electricity and heat sources. We use the year 2050 as a reference point, as it aligns with most global net-zero targets and represents a stage at which DAC technologies are expected to have matured, benefiting from technological learning, large-scale deployment, and reduced capital costs. Building upon previous research, we simulate the hourly performance of an amine-functionalized adsorption process and an electrified liquid solvent process by utilizing process-based data (An et al., 2022; Sendi et al., 2022; McQueen et al., 2021). We develop a techno-economic optimization model that incorporates region-averaged weather-dependent hourly performance data for DAC with region-specific renewable potential and detailed techno-economic parameters. This model calculates the levelized cost of DAC (LCOD) for fully electrified and hybrid heat supply options across 3827 subnational regions globally. Our study provides these contributions to the literature on DAC techno-economics:

- Covers L-DAC and S-DAC technologies, explicitly accounting for documented process-level responses to temperature and humidity within data-supported operating ranges.
- Produces spatially explicit global maps of DAC cost and deployment potential, enabling direct comparison of regional feasibility under fully renewable operation.
- Identifies cost-effective, technology-specific regions capable of supporting gigaton-scale CO_2 capture, providing actionable guidance for strategic global DAC deployment.

By coupling weather-dependent DAC performance with geographically resolved renewable energy systems and water costs, the analysis moves beyond site-agnostic or static cost estimates and provides a consistent global benchmark for strategic gigaton-scale capture by 2050. In light of emerging international carbon market mechanisms under Article 6 of the Paris Agreement and ongoing discussions about integrating DAC credits into systems such as the EU ETS (UNFCCC, 2015), this global assessment contributes to the policy debate by identifying cost-effective regions for potential cross-border deployment and credit generation. This paper is organized as follows: Section 2 details our methodology, including weather and DAC performance data processing, techno-economic data acquisition, and global renewable energy potential. Section 3 presents the results, including global techno-economic DAC potential, merit order plot and cost sensitivity, followed by discussions and conclusions in Section 4.

2. Methods

This study models the global potential of the L-DAC and S-DAC, evaluating the levelized costs across regions to identify the key cost drivers and cost-efficient technology pathways. For our analysis, we apply the ETHOS.FINE energy system modeling framework (Fig. 1) (Klütz et al., 2025), which integrates energy sources, conversion, and storage with a detailed DAC module whose hourly productivity and energy demand constraints shape the model behavior. We conduct a merit-order analysis to identify the most economically viable regions using a mid-range estimate of 2 $GtCO_2$, within the projected global DACS deployment range of 0.5 – 5 $GtCO_2$ in 2050 (IPCC, 2022; IEA, 2022; Fuss et al., 2018). To account for the uncertainty of the future evolution of DAC technologies and their associated energy demand, we present three cost scenarios: optimistic, baseline, and pessimistic. These scenarios capture a plausible range of techno-economic outcomes based on projected learning rates and system integration maturity. This approach enables assessment of the robustness of DAC performance and cost across contrasting development pathways and highlights the sensitivity of large-scale deployment to technological and systemic uncertainties.

The integrated model first calculates the maximum technical DAC potential in a region based on the availability of renewable energy resources. The estimation of technical DAC potential is constrained by land availability for renewable energy deployment. The underlying renewable energy potential datasets implicitly incorporate land-use exclusions, including areas such as settlements, infrastructure, water bodies, protected areas, and forests. These criteria encompass a large number of parameters. For instance, the geothermal potential used in this study assumes a minimum distance of 300 m to settlements due to noise constraints and excludes protected areas, regions with high water scarcity due to plant water demand, and areas with slopes exceeding 17° (Franzmann et al., 2025). A comprehensive description of all criteria can be found in the literature from which these potentials are derived (Franzmann et al., 2025; Franzmann et al., 2025; IEA, 2024; Winkler et al., 2025). In the second step, the model performs cost optimization, assuming a DAC demand of 1% of its maximum technical potential. This fractional demand does not represent an actual deployment level; rather, it provides a consistent way to allocate DAC capacity across

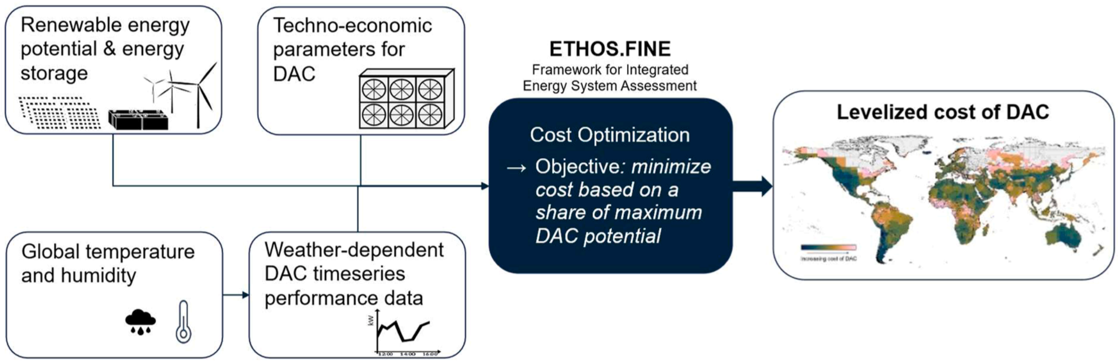

Fig. 1. Integrated techno-economic framework for DAC potential assessment.

regions in the absence of established regional DAC deployment targets. Selecting a fixed share of each region's maximum potential ensures comparability across regions and avoids imposing arbitrary or exogenous regional demand assumptions. The choice of 1% is a modeling assumption that functions solely as a scaling factor. Using any similarly small fractional share results in comparable spatial cost patterns, as most regions operate far below renewable-resource saturation. During optimization, the capacity of each component and its operation for 8760 hours per year are optimized to minimize the total annual system cost (TAC). We derive the LCOD for each region by dividing the TAC by the sum of captured CO_2 mass in each hour of the year, $op_{CO2,t}$.

$$LCOD = \frac{TAC}{\sum_{t=0}^{T} op_{CO2,t}} \tag{1}$$

2.1. Weather data and DAC performance parameterization

As no reliable, high-resolution global weather dataset is available for 2050, we use 2018 as a representative reference year. This approach aligns with a study by IRENA, which considers 2018 to be broadly representative of the 2010 – 2020 period (IRENA, 2022). This period was characterized by relatively moderate weather anomalies, making 2018 suitable for global, comparative assessments of future energy systems and weather-dependent technologies. We used hourly weather data from ERA5 reanalysis dataset with a spatial resolution of 0.25° x 0.25° (C3S, 2018). Since relative humidity data are not directly provided by ERA5, we calculated it from dewpoint temperature and air temperature using the Sonntag formula (Sonntag, 1990; Wexler, 1976). This approach ensured consistency in calculating relative humidity across the globe (see Equations 1 – 3 in the *Supplementary Information*). The weather data are spatially clipped to each subnational region. Depending on the size and geometry of the region, this results in one or multiple grid cells per region. For each region, the weather variables are aggregated by averaging across all intersecting grid cells to yield a single representative hourly time series. DAC performance is then evaluated using the resulting aggregated time series. While this approach avoids biases associated with selecting a single representative grid cell, it also smooths spatial variability within each region, which may introduce additional uncertainty due to nonlinear relationships between DAC performance and ambient conditions.

We used process performance data from previous studies to accurately model the influence of temperature and relative humidity conditions for an electrified calcination-based L-DAC and a steam-assisted temperature vacuum swing adsorption S-DAC (see Section 1 of the *Supplementary Information*) (An et al., 2022; Sendi et al., 2022; McQueen et al., 2021). The system boundary of the performance models includes CO_2 capture and compression to 150 bar. The performance data are derived from process-based models for ambient temperature and relative humidity ranges of 0 – 40 °C and 10 – 90 % for L-DAC, and 1 – 50 °C and 5 – 100 % for S-DAC (An et al., 2022; Sendi et al., 2022). Within these ranges, region-specific average hourly temperatures and relative humidities are interpolated to estimate the relative productivity, energy demand, and water consumption of DAC in each region. Since high air temperatures do not hinder L-DAC operation, and due to the lack of data above 40 °C, we assume constant performance between 40 °C and 50 °C (Brooks et al., 2024; Kucka et al., 2002). This assumption enables the model to represent regions with extreme hourly temperatures without artificially constraining L-DAC deployment. Furthermore, the modeled minimum operating temperatures for L-DAC and S-DAC are set at 0 °C and −15 °C, respectively. These constraints reflect current process and material limitations and ensure realistic operation by excluding periods in which capture performance or equipment integrity would be compromised.

Although a 1.1 mol/L KOH solution can depress the freezing temperature to approximately −4 °C, a minimum operating temperature of 0 °C is maintained for L-DAC, as process data are unavailable at sub-zero temperatures (Shorey and Abdulla, 2024; Brooks et al., 2024). S-DAC can operate below 0 °C, with its device components insulated to withstand sub-zero temperatures (Jajjawi et al., 2026; Elfving et al., 2017). However, process model data on the adsorption capacity and mass transfer of the sorbent at sub-zero temperatures remain scarce, with only a few recent studies exploring a limited range of conditions (Sendi et al., 2022; Jajjawi et al., 2026; Cai et al., 2024). This limits the ability to validate model performance robustly across the full range of cold climates considered in this work. Therefore, we assume the same performance below 1 °C down to −15 °C. This simplification neglects the potential reduction in mass transfer kinetics at lower temperatures, which could lead to longer cycle times and reduced productivity, and could therefore result in an underestimation of capture costs in cold regions (Jajjawi et al., 2026; Spreng et al., 2026). Restricting L-DAC operation below 0 °C reduces annual operating hours in cold climates. However, this effect is regionally limited and does not significantly impact global cost trends. Lastly, the relative productivity of both technologies is determined by the actual productivity under varying weather conditions, divided by the nominal productivity under global-average conditions. Relative productivity provides a baseline for comparing the productivity of each technology as a function of temperature and relative humidity. Further details on the simulation of weather-dependent performance data for DAC are described in our previous study (Wenzel et al., 2025).

2.2. Global renewable energy potential and configuration

The renewable energy technologies and potentials we considered are onshore wind, horizontal single-axis tracking open-field photovoltaics (HSAT OFPV), enhanced geothermal systems (EGS) (see (Franzmann et al., 2025)), and concentrated solar power (CSP) (see (Franzmann et al., 2025)). The wind and HSAT OFPV potential, as well as the hourly-resolved supply profiles, are based on analyses conducted in cooperation with the International Energy Agency for their Global Hydrogen Review 2024 (IEA, 2024; Winkler et al., 2025). The CSP potential and hourly generation profiles are based on literature datasets using physical models from the National Renewable Energy Laboratory and the German Aerospace Center translated into analytical formulations, combined with ERA5 weather data and land eligibility constraints to generate location-specific time series (Franzmann et al., 2025). Further details on the simulation of wind, HSAT OFPV, and CSP are available in the Renewable Energy Simulation Toolkit for Python (ETHOS.RESkit) (Ryberg, 2019; Winkler et al., 2025). Geothermal potentials are derived from a global, site-specific framework combining land eligibility, subsurface temperature modeling, and physics-based reservoir models such as the Gringarten approach to estimate realistic plant output and costs under geological and operational constraints (Franzmann et al., 2025). Renewable energy generation is represented by using clustered resource profiles, which better preserve temporal variability and co-variation in generation patterns within each region. These profiles are derived from raw weather data using ETHOS.RESkit (Ryberg, 2019; Winkler et al., 2025) at the grid-cell level and then aggregated into representative clusters. Three time-series clusters are assigned per region for HSAT OFPV, CSP, and EGS, while ten clusters are used for onshore wind to reflect its stronger spatial variability. These numbers were selected based on recommendations from literature (Franzmann et al., 2025), which emphasize the need for technology-specific clustering to capture key system interactions while maintaining computational tractability. This approach is particularly important for variable renewables, as system costs depend on the temporal alignment of generation and storage requirements.

We also consider energy conversion components, such as CSP power plants, electric heaters, and heat pumps, to facilitate the conversion of electricity to heat or vice versa. We model the heat pump by calculating an hourly, region-specific coefficient of performance based on the air temperature, assuming a second-law efficiency of 50% (Wenzel et al., 2025). Additionally, our analysis includes energy storage, specifically lithium-ion battery storage for electricity, high-temperature thermal storage for CSP-based heat supply, and low-temperature thermal storage for process heat integration. Furthermore, we assume a generic water source with unlimited potential to supply water for L-DAC. We derive an average, country-specific levelized cost of water for 2050 based on literature (Caldera and Breyer, 2020). Data on the levelized cost of water were available for 175 countries. For the remaining countries, we use the global average estimate.

Fig. 2 shows the full electric and hybrid energy supply configurations defined for DAC. For L-DAC, the thermal energy demand is split between the CSP and electric calciner in the hybrid configuration. The CSP is used to provide low to intermediate temperature heat, preheating the $CaCO_3$ stream from ambient conditions to approximately 380 °C. The remaining high-temperature heat required for calcination is supplied by the electric calciner. To quantify the relative contributions of CSP and the electric calciner, the sensible heat demand for $CaCO_3$ was divided into two temperature intervals: ambient to 380 °C for CSP supply and 370 – 900 °C for electric heating. The heat required in each interval was estimated using literature values of the average heat capacity of $CaCO_3$ (Jacobs et al., 1981), and the fractional energy contributions were calculated as the ratio of the heat demand in each interval to the total sensible heat requirement. This split reflects a simplified representation of current CSP integration concepts. Although higher-temperature CSP configurations are technically feasible, large-scale deployment is subject to increased system complexity and relatively limited commercial maturity. Heat recovery within the process is included and cascaded to lower-temperature units, such as the steam slaker, consistent with conventional process integration strategies (Keith et al., 2018). While we consider an electrified calcination for L-DAC, substantial development is necessary to scale up today's smaller units for large-scale operation for 2050-scale plants (McQueen et al., 2021). A simplified process flow diagram and description of the thermal energy split are provided in Section 1 and 2 of the *Supplementary Information*. This energy configuration distinction enables an assessment of how various

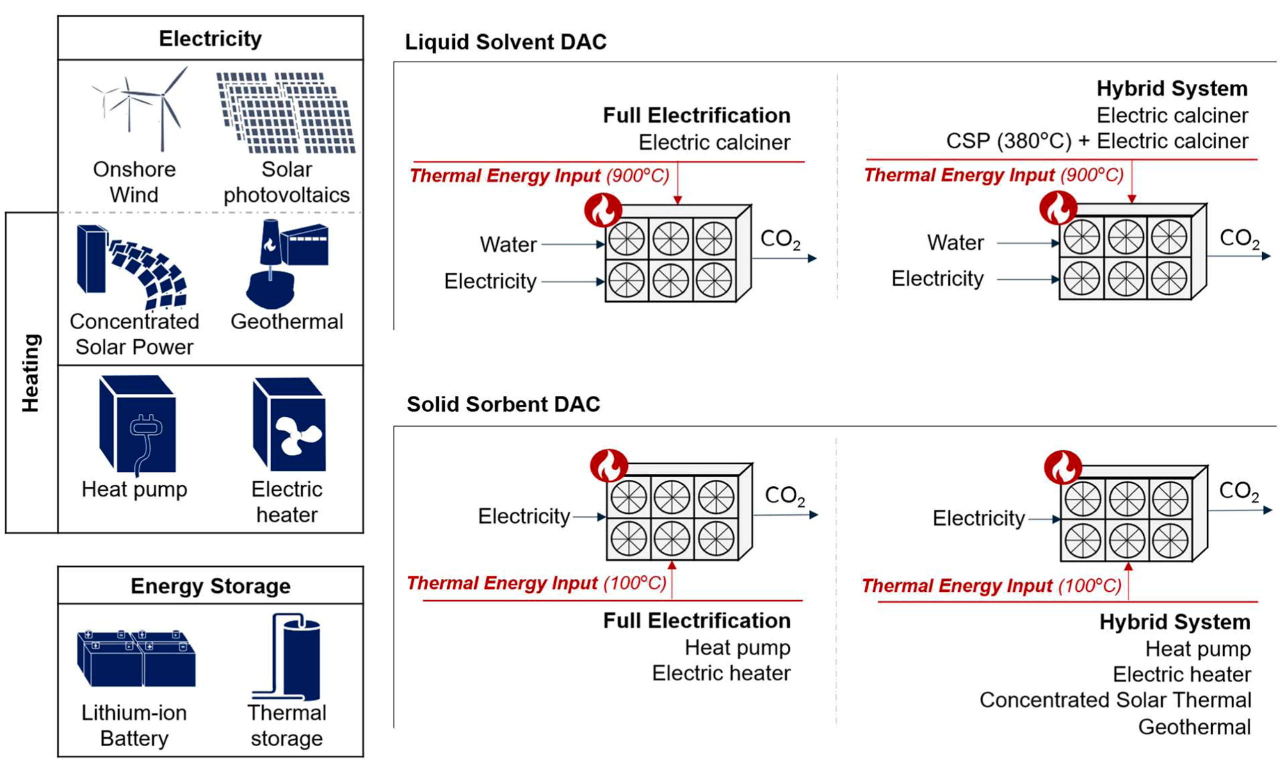

Fig. 2. Definition of energy supply configurations for L-DAC and S-DAC. In the electric configuration, all heat demand is met through electrically driven heating technologies (e.g., an electric calciner for L-DAC and a high-temperature heat pump for S-DAC). In the hybrid configuration, renewable heat sources from geothermal and CSP are integrated to supply all or part of the thermal demand directly.

energy supply pathways impact system performance and costs.

2.3. Techno-economic data

We obtained the techno-economic parameters for DAC through a systematic literature review, focusing on studies that provided parameters for 2050 or for a gigaton-scale capture. The parameters obtained include capital cost, operating cost, weighted average cost of capital (WACC), economic lifetime, and utilization factor. The selected studies incorporate technological learning and scale effects through various established methodologies. For example, multi-component experience curves have been applied to differentiate learning rates across system components rather than assuming a uniform system-wide rate (Sievert et al., 2024). Meanwhile, bottom-up first-of-a-kind cost estimates have been combined with top-down learning curve projections to derive future costs (Young et al., 2023). In contrast, the IEAGHG assessment adopts a more conservative stance, highlighting the uncertainty of long-term learning projections and incorporating learning rates primarily within sensitivity analyses (IEAGHG, 2021). We therefore do not construct an independent long-term cost projection, but instead synthesize forward-looking estimates and represent them using quartile and median values to define optimistic, baseline, and pessimistic cases. This allows us to transparently reflect the spread of reported expectations in the literature while avoiding reliance on a single assumed learning rate. Fig. 3 presents the literature-based CAPEX and OPEX values used as the basis for the cost estimates in this study.

As literature data generally shows significant variations in stated cost estimates for DAC, mostly reflecting differences in system boundaries, assumptions, and technology maturity, we define our system boundary to cover DAC up to 150 bar compression. Furthermore, we discount the DAC capital costs using a WACC of 10 % over a lifetime of 25 years, consistent with literature assumptions for 2050 (Sievert et al., 2024; IEAGHG, 2021; Realmonte et al., 2019; Hanna et al., 2021; Young et al., 2023). No additional financial learning or endogenous reduction in financing risk is considered, meaning that further potential declines in the cost of capital are not captured (Egli et al., 2018). Additionally, we added compressor costs to the capital costs in publications that did not originally consider CO_2 compression, and based on the stated cost in the literature (Keith et al., 2018). To ensure comparability across sources, we converted all cost values to real 2024 € using exchange rates and inflation data (European Central Bank, 2024a, 2024b). No additional inflation projection to 2050 was applied. Table 1 presents the median values of capital and operating costs from the literature, along with other relevant parameters used to model DAC. Sorbent and solvent costs are represented as variable OPEX (IEAGHG, 2021; Young et al., 2023). For S-DAC, sorbent costs are higher than the corresponding solvent costs in L-DAC, reflecting both the higher cost of solid sorbent and the need for periodic replacement. While this approach accounts for sorbent replacement in operating costs, degradation effects on system performance are not explicitly modeled. We present the upper and lower quartiles in Table 1 and use these to run pessimistic and optimistic scenarios. Further, detailed techno-economic parameters for the energy sources, conversion, and storage components are provided in Table S1 (see *Supplementary Information*).

3. Results

3.1. Global techno-economic potential of direct air capture technologies

We present the cost optimization results for L-DAC and S-DAC on a single global map (Figs. 3A and 3B), illustrating the more cost-effective technology across all regions in the electric and hybrid configurations. Across both configurations, tropical regions tend to be cost-optimal for L-DAC, while temperate, cold, and polar regions are better suited for S-DAC. In arid regions, L-DAC consumes more water due to higher evaporation in the air contactor, which must be replaced more frequently, increasing the LCOD. The high water cost contribution reaches 8 – 12% of the LCOD in countries such as Niger, Chad, Sudan, Algeria, Yemen, Iran, and Turkmenistan, generally making S-DAC the more cost-effective option. L-DAC becomes favorable only in arid locations where the levelized cost of water is comparatively low. Additionally, L-DAC tends to be more expensive as operations move northward due to unfavorable sub-zero conditions that limit its operation.

In the electric configuration, regions in Africa and South America offer the lowest costs for both DAC technologies, reaching 173 €/tCO_2 in Colombia for L-DAC and 205 €/tCO_2 in Western Sahara for S-DAC. These low costs are primarily driven by abundant, inexpensive wind resources, which lower overall energy costs. Across most regions, S-DAC is more cost-competitive than L-DAC. However, L-DAC has lower costs in Australia, South America, and the Middle East and Northern Africa. Additionally, regions in southern Europe, Asia, and North America, particularly Spain, Portugal, Italy, Greece, Turkey, Japan, and the USA (Texas, Louisiana, Florida), have lower levelized costs for L-DAC. The northernmost point at which L-DAC remains more cost-effective than S-DAC occurs in Ireland. The coastal regions of Ireland typically have high humidity, which contributes to higher thermal demand and levelized costs of S-DAC. However, the cost difference between the two DAC technologies within these regions is only about 2 – 5 €/tCO_2.

Switching from full electrification to a hybrid system reduces the LCOD (Fig. 4C). This cost reduction stems from integrating direct

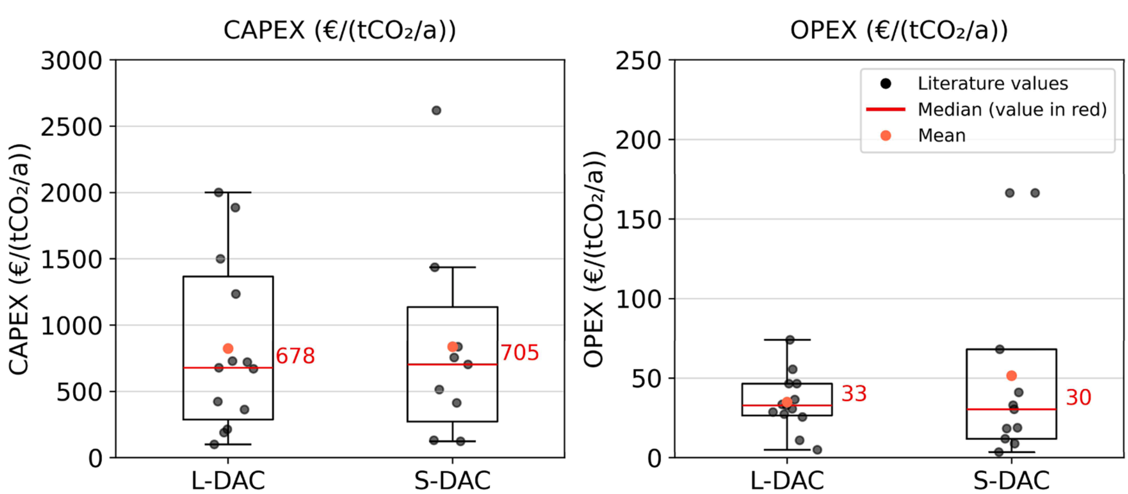

Fig. 3. Literature-based estimates of capital and operating expenditures for L-DAC and S-DAC in 2050 (Sievert et al., 2024; IEAGHG, 2021; Fasihi et al., 2019; Realmonte et al., 2019; Pett-Ridge et al., 2023; Hanna et al., 2021; Fuhrman et al., 2021; Young et al., 2023).

Table 1

Techno-economic assumptions for DAC in the year 2050. This table reports cost and performance parameters for DAC. Performance parameters are region-specific and derived from spatially averaged weather conditions (see Figures S5 – S6). Energy supply costs are determined endogenously through the optimization of renewable energy and storage systems, whose techno-economic assumptions are provided in Table S1 of the Supplementary Information.

Parameters Liquid solvent DAC	Unit	Value	Source/notes
CAPEX	(€/tCO_2/a)	1368 – Q3 678 – Median 290 – Q1	Lower (Q1) and upper (Q3) quartiles are used for the optimistic and pessimistic cases, respectively (Sievert et al., 2024; IEAGHG 2021; Fasihi et al., 2019; Realmonte et al., 2019; Pett-Ridge et al., 2023; Hanna et al., 2021; Fuhrman et al., 2021; Young et al., 2023)
Fixed OPEX	(€/tCO_2/a)	46 – Q3 33 – Median 27 – Q1	Lower (Q1) and upper (Q3) quartiles are used for the optimistic and pessimistic cases, respectively (Sievert et al., 2024; IEAGHG, 2021; Fasihi et al., 2019; Realmonte et al., 2019; Pett-Ridge et al., 2023; Hanna et al., 2021; Fuhrman et al., 2021; Young et al., 2023)
Variable OPEX	(€/tCO_2)	1.4 - 3	Includes solvent costs only. Upper bound value assumes chemical makeup requirement of 3 kg KOH + $CaCO_3$ per tCO_2 captured and is used for the pessimistic case (IEAGHG, 2021; Young et al., 2023)
Relative productivity	(-)	0.7 – 1.3	Derived from literature-based, weather-dependent productivity (An et al., 2022). Relative productivity is the ratio of actual to nominal productivity under global-average conditions.
Specific electricity demand	(MWh/tCO_2)	1.9 – 2.4	Literature-based, weather-dependent demand (An et al., 2022; McQueen et al., 2021). Within the range of 1 $GtCO_2$/a scale plant (Young et al., 2023), NOAK Liquid DACCS (IEAGHG, 2021), 1 $MtCO_2$/a scale plant (Keith et al., 2018)
Specific water demand	(tH_2O/tCO_2)	1 – 24	Literature-based, weather-dependent demand (An et al., 2022)
Solid sorbent DAC			
CAPEX	(€/tCO_2/a)	1137 – Q3 705 – Median 273 – Q1	Lower (Q1) and upper (Q3) quartiles are used for the optimistic and pessimistic cases, respectively (Sievert et al., 2024; IEAGHG, 2021; Fasihi et al., 2019; Realmonte et al., 2019; Pett-Ridge et al., 2023; Hanna et al., 2021; Fuhrman et al., 2021; Young et al., 2023)
Fixed OPEX	(€/tCO_2/a)	68 – Q3 30 - Median 12 – Q1	Lower (Q1) and upper (Q3) quartiles are used for the optimistic and pessimistic cases, respectively (Sievert et al., 2024; IEAGHG 2021; Fasihi et al., 2019; Realmonte et al., 2019; Pett-Ridge et al., 2023; Hanna et al., 2021; Fuhrman et al., 2021; Young et al., 2023)
Variable OPEX	(€/tCO_2)	39 - 74	Includes sorbent costs only. Lower-bound value assumes a sorbent replacement rate of three years and is used for the optimistic and baseline cases (Young et al., 2023). Upper bound value assumes a replacement rate at 7.5 kg of sorbent per tCO_2 captured and is used for the pessimistic case (IEAGHG, 2021)
Relative productivity	(-)	0.5 – 1.1	Derived from literature-based, weather-dependent productivity (Sendi et al., 2022). Relative productivity is the ratio of actual to nominal productivity under global-average conditions.
Specific electricity demand	(MWh/tCO_2)	0.2 – 0.9	Literature-based, weather-dependent demand (Sendi et al., 2022)
Specific thermal demand	(MWh/tCO_2)	1.9 – 5.1	Literature-based, weather-dependent demand (Sendi et al., 2022). In the optimistic case, thermal demand is reduced by 45% in line with projected efficiency in (IEAGHG, 2021; Young et al., 2023)

geothermal and CSP heat into the energy mix. The integration lowers the global levelized cost of S-DAC, reaching 176 €/tCO_2 in Iceland. Similar cost reductions of 13 – 32% are observed in other regions with accessible low-cost geothermal heat, including Mexico, Japan, China, and Chile. Since only about 35% of L-DAC's heat can be supplied by CSP alone, the levelized cost of L-DAC decreases by up to 12% or less in regions with high CSP potential, such as Brazil, South Africa, Australia, and the Middle East and Northern Africa. The hybrid configuration not only offers lower costs and greater deployment potential but also shifts regional preferences between DAC technologies, favoring S-DAC in areas such as Indonesia and southeastern Australia, where low-cost geothermal heat is available. As both technologies rely heavily on heat for regeneration, access to a low-cost heat source is vital to reducing costs.

Comparing the two energy configurations, the integration of direct geothermal and CSP heat in the hybrid configuration leads to a 5 – 8% reduction in global median LCOD, from 284 €/tCO_2 to 271 €/tCO_2 for L-DAC and from 275 €/tCO_2 to 254 €/tCO_2 for S-DAC. This reduction highlights the importance of low-cost heat for future DAC deployment. While weather conditions impact the productivity and energy demand (see Figures S4 and S5 in the *Supplementary Information*), differences in renewable energy availability and type translate into varying energy costs, which in turn drive regional cost differences across both technologies. We further elaborate on the results for the hybrid configuration, given its lower costs and greater DAC potential.

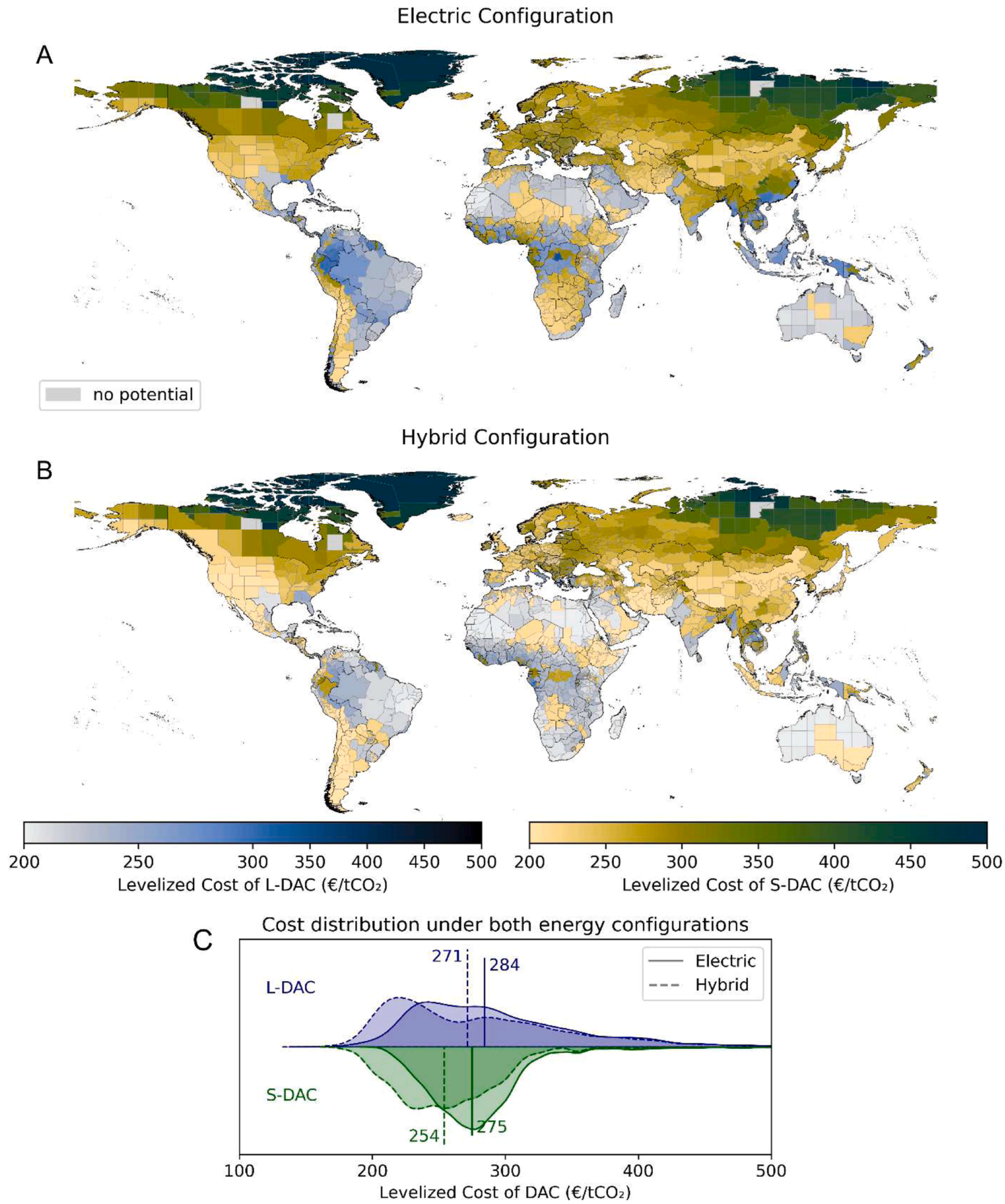

Fig. 4. Global levelized cost of DAC by 2050 under two energy supply configurations. A) Global cost map of DAC under the electric configuration, B) Global cost map of DAC under the hybrid configuration, C) Global cost distribution for both DAC technologies under the electric and hybrid configuration. The whitish and blue regions in the global map cover areas where the levelized cost of L-DAC is lower, while the yellow and green regions represent areas where S-DAC has a lower levelized cost.

3.2. Levelized costs and energy mix for representative regions

To evaluate the main cost drivers of DAC, Fig. 5 compares cost components across representative low- and high-cost regions. In all four low-cost regions (Fig. 5A), energy costs account for only a small share of the total levelized cost due to the availability of low-cost renewable energy. As a result, 85 - 88% originates from S-DAC capital and operating costs. The low-energy contribution in these regions stems from geothermal heat (Fig. 5B), which provides a stable, inexpensive source of thermal energy. While geothermal integration can substantially lower DAC costs in some areas, it does not guarantee similar benefits in all regions, as costs scale with drilling depth (Franzmann et al., 2025). In contrast, the three highest-cost regions show markedly higher energy costs. In these regions, the system relies more heavily on electrically supplied heat due to the lack of direct renewable heat sources. As a result, energy costs account for at least 43% of LCOD in these regions. Moreover, extreme cold temperatures in RUS (Russia, Sakha) and CAN (Canada, Nunavut) limit DAC operations and reduce the efficiency of heat pumps, thereby increasing the LCOD. The low-cost regions of L-DAC (Fig. 5C) are generally characterized by high CSP and steady wind potential, enabling a continuous and low-cost energy supply. In contrast, regions with limited CSP potential, such as VNM (Vietnam, Thái Nguyên), LBR (Liberia, Bomi) and HKG (Hong Kong, Sai Kung), rely on full electric calcination, exhibiting higher overall costs.

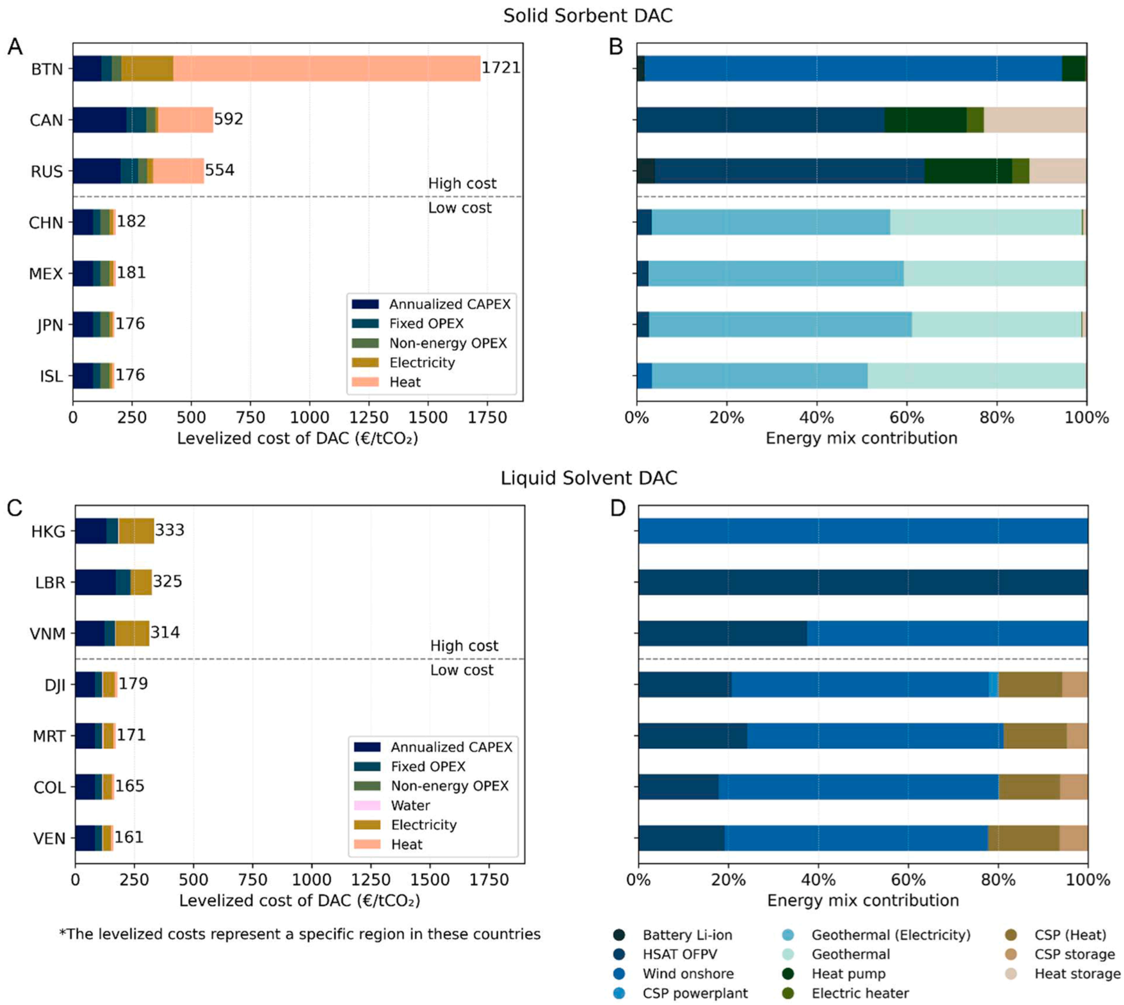

Fig. 5. Cost component for representative DAC regions based on the hybrid energy configuration. A-B) Levelized cost and energy mix contribution of S-DAC, and C-D) Levelized cost and energy mix contribution of L-DAC. The regions with the lowest and highest average costs per country are shown. Electricity components are on the left side of the energy mix contribution graph, while heat components are on the right. The regions correspond to the first administrative level in each country: ISL (Iceland, Vesturland), JPN (Japan, Kagoshima), MEX (Mexico, Sinaloa), CHN (China, Shanghai), RUS (Russia, Sakha), CAN (Canada, Nunavut), BTN (Bhutan, Trongsa), VEN (Venezuela, Nueva Esparta), COL (Colombia, La Guajira), MRT (Mauritania, Dakhlet Nouadhibou) DJI (Djibouti, Obock), VNM (Vietnam, Thái Nguyên), LBR (Liberia, Bomi) and HKG (Hong Kong, Sai Kung).

The capital and operating costs of DAC are the dominant contributors to the LCOD across both technologies, together accounting for 45 – 90% of the total cost (See Figures S8, S10, S12, and S14 in the *Supplementary Information*). For S-DAC, this share is typically higher at around 65 – 90%, primarily due to higher sorbent costs. In contrast, L-DAC shows a lower capital and operating cost share of about 45 – 65%, largely due to its inexpensive solvent. However, in arid regions, increased water replacement needs can substantially elevate the levelized cost of L-DAC, narrowing the cost gap between the two technologies.

It is important to highlight that in this study, we treat financing costs as fixed to focus on the technical and weather impacts on DAC technologies. However, the levelized costs of both DAC and renewable energy are highly sensitive to financing conditions (Sendi et al., 2024; Egli et al., 2019; Steffen et al., 2025). To reduce overall costs, large-scale deployment will therefore require not only continued advances in process efficiency and reductions in material and equipment costs but also improved access to low-cost financing. This highlights the importance of stable policy frameworks, risk mitigation instruments, and access to low-cost capital to enable large-scale DAC deployment, particularly in emerging markets with higher investment risk.

3.3. *Global merit order of direct air capture*

Building on these regional insights, the global merit order, which is constructed from the cost-optimal combination of S-DAC and L-DAC, provides a broader perspective on how these cost variations translate into cumulative capture potential at different cost levels. The global merit order of DAC at a 1% share of the maximum DAC potential shows a cumulative potential of approximately 33 $GtCO_2$. As shown in Fig. 6, a fully renewable DAC system can achieve a global potential of 2 $GtCO_2$ at costs below 195 €/tCO_2. We use 2 $GtCO_2$ as a representative mid-range value within the projected global DAC deployment range of 0.5 – 5 $GtCO_2$ by 2050 (IPCC, 2022; IEA, 2022; Fuss et al., 2018). The lowest costs are observed in Australia, Iceland, Japan, Chile, China, Mexico, and parts of South America, South East Asia, and the Middle East and Northern Africa, where favorable weather conditions and high-quality renewable resources enhance DAC performance. Regions in Australia, Iceland, Chile, China, Japan, Mexico, and Southeast Asia are cost-optimal for S-DAC, while much of South America, and the Middle East and Northern Africa are suited for L-DAC. Regions in Europe and the United States achieve costs in the range of 195 – 400 €/tCO_2. Conversely, cold regions within Russia, Canada, Greenland, and small islands in Southern Africa exhibit the highest levelized costs, ranging

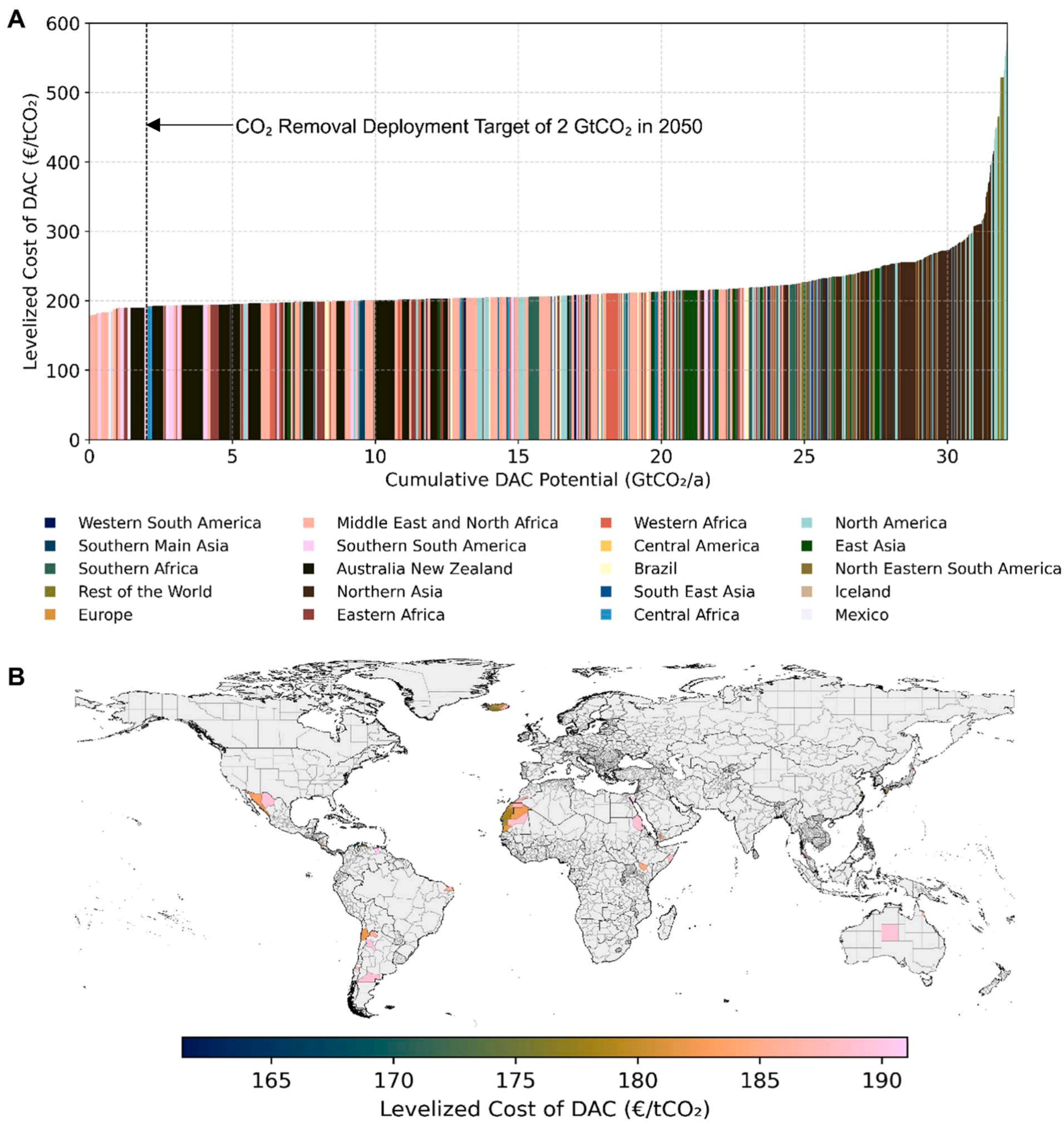

Fig. 6. Global merit order of DAC in 2050 based on the hybrid energy configuration. A) Cumulative DAC potential versus LCOD by world region (see region grouping in Section 4 of the Supplementary Information). The projected global DACS demand in 2050 at 2 $GtCO_2$ corresponds to only a small fraction of the total techno-economic DAC potential identified in this study. Each colored segment represents a world region, highlighting regional differences in both cost and DAC potential B) Global map of LCOD at a deployment level of 2 $GtCO_2$ showing the spatial distribution of cost-optimal regions.

from 400 – 1720 €/tCO_2. This reflects limited renewable potential and suboptimal conditions for DAC operation in these regions. These results demonstrate that the technical DAC potential based on renewable energy availability exceeds the expected global demand. Within the scope of this study, the levelized cost of DAC is likely to be a key constraint on large-scale deployment. However, other factors, such as CO_2 transport and storage infrastructure, supply chains, and deployment rates, will also play a major role but are not assessed in this study. Furthermore, the significant regional cost heterogeneity underscores the importance of international trade and infrastructure development to leverage low-cost capture regions and build cost-effective global DAC supply chains. Identifying regions with the lowest DAC cost can also support the implementation of Article 6 under the Paris Agreement (UNFCCC, 2015), by informing the design of international carbon market mechanisms and enabling cost-efficient cross-border cooperation to achieve net removal targets.

3.4. Cost sensitivity under pessimistic and optimistic cases

Given the uncertainty in reported CAPEX and OPEX values across the literature, we assessed both pessimistic and optimistic cost cases based on upper and lower bound values derived from literature reported ranges, as shown in Fig. 7. The pessimistic case reflects upper-bound cost estimates for key cost parameters, including capital, fixed, and variable operating costs. Under these assumptions, the global median levelized cost remains high, with S-DAC reaching 390 €/tCO_2 and L-DAC approximately 392 €/tCO_2. These elevated costs are driven by higher CAPEX and OPEX assumptions. These results suggest that large-scale DAC deployment may remain economically challenging if costs remain near the upper range of current literature estimates. In contrast, the optimistic case applies lower-bound cost assumptions from literature, together with a 45% reduction in thermal demand for S-DAC. The reduction is based on NOAK system projections reported in the literature (IEAGHG, 2021; Young et al., 2023), which incorporate expected

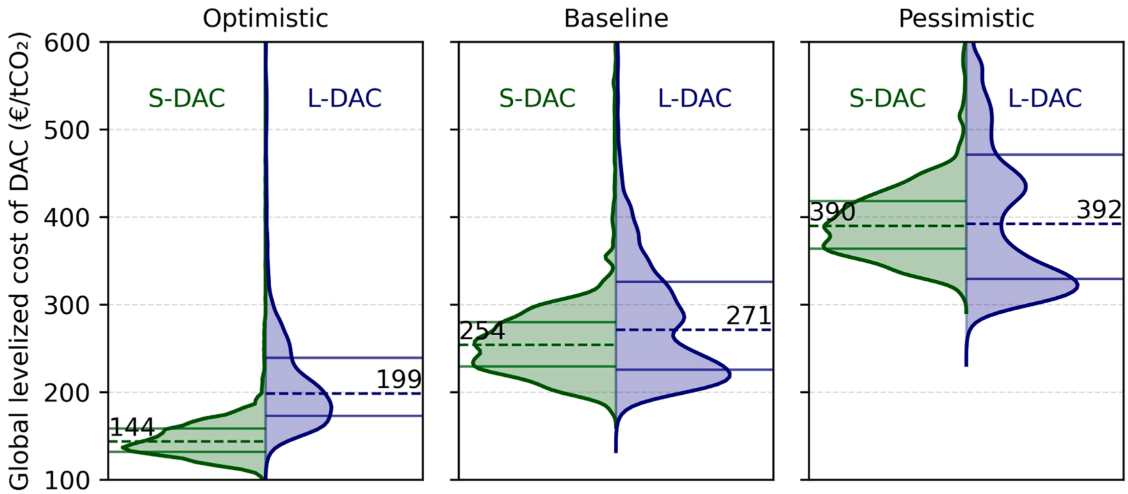

Fig. 7. Global levelized cost of DAC for optimistic, baseline, and pessimistic scenarios. These scenarios reflect parameter uncertainty, including CAPEX, OPEX, and energy demand. The optimistic and pessimistic cases represent the lower and upper bounds of cost and performance parameters reported in the literature, respectively, while the baseline case corresponds to median values. The dashed lines represent the median costs, while the straight lines correspond to the upper and lower quartiles. Global merit order plots for the individual DAC technologies under the pessimistic and optimistic cases are shown in Figures S15 – S18 of the Supplementary Information.

improvements in process integration, heat recovery, and sorbent performance. Under these assumptions, S-DAC achieves costs as low as 100 €/tCO_2 in Iceland, with an average specific thermal demand of 1.43 MWh/tCO_2. The median S-DAC cost significantly falls below L-DAC's under these conditions. No reduction in energy demand is assumed for L-DAC, as its solvent regeneration process is relatively mature and constrained by thermodynamic limits. Overall, these results highlight that DAC cost estimates are highly sensitive to literature-based parameter ranges. The relative cost competitiveness of L-DAC and S-DAC depends strongly on whether costs evolve towards the lower or upper bounds reported in the literature.

In addition to the scenario-based analysis, we evaluated how sensitive DAC costs are to key individual parameters (see Figure S19 in the *Supplementary Information*). The results demonstrate that DAC costs are sensitive not only to cost assumptions and energy demand but also to financial and operational parameters, such as the WACC and plant utilization factor. For the representative low-cost regions identified in Fig. 5, varying the WACC by ±50% from a baseline of 10% results in cost changes of approximately 16 – 20%. Furthermore, reducing the utilization factor from a baseline of 90% to 60% leads to a larger cost increase of 23 – 31%. While these parameters have a notable impact on levelized costs, the results indicate that literature-based cost assumptions remain the dominant source of uncertainty.

4. Discussion and conclusions

Our results demonstrate the critical importance of considering region-specific renewable energy potential and weather conditions when selecting sites for DAC. This study provides a comprehensive framework for evaluating the spatial variability of DAC costs at scale by integrating techno-economic analysis with a globally resolved, high-resolution assessment of renewable energy availability and weather-dependent performance. Global levelized costs of DAC range from 160 €/tCO_2 to 1720 €/tCO_2 by 2050, with S-DAC typically cost-optimal in temperate, cold, and arid regions and L-DAC in tropical regions or arid regions with a low levelized cost of water. The energy supply configuration of both DAC systems contributes to minimizing LCOD, as direct renewable heat sources provide lower cost than electrically driven heating technologies. Hybrid heating lowers the global median levelized cost of DAC by up to 8%, and by as much as 32% in geothermal-rich regions. By prioritizing cost-optimal locations, our results show that levelized costs below 195 €/tCO_2 in 2050 are feasible for an annual DAC potential of 2 $GtCO_2$, particularly in regions such as Australia, Chile, Iceland, and parts of China, Mexico, Southeast Asia, and the Middle East and North Africa.

This spatially explicit perspective highlights the importance of strategic siting for enabling cost-effective large-scale deployment and may provide a basis for international cooperation under Article 6 of the Paris Agreement. Identifying low-cost regions can facilitate cross-border mitigation and support the potential integration of carbon removal credits into mechanisms such as the EU Emissions Trading System (Rickels et al., 2021). Despite these opportunities, achieving a cost threshold of around 100 €/tCO_2 with DACS appears very unlikely by 2050, even under optimistic assumptions. Under upper-bound cost assumptions, DAC costs could remain above 300 €/tCO_2, indicating that large-scale deployment could remain economically challenging.

Achieving climate targets for 2050 will require addressing residual and hard-to-abate emissions, for which CDR, including DAC, is expected to play a leading role alongside conventional mitigation measures. This study contributes to this discussion by providing a globally consistent, techno-economic assessment of DAC deployment potential that explicitly links capture costs to spatial variations in weather conditions, renewable energy availability, and water costs. Although DAC is a promising CDR option, its large-scale deployment depends on continued research and innovation, alongside rapid scaling and strategic global deployment, to minimize its cost and energy requirements. L-DAC and S-DAC present different challenges and opportunities due to the interactions between air and the capture material used, as well as their respective regeneration temperatures and energy requirements. While the decision on where to site DAC requires evaluating interrelated geospatial factors, we provide a framework for strategically deploying DAC facilities by prioritizing regions with favorable weather conditions and low-cost energy. As such, the results provide a foundation for integrating DAC into broader energy system planning and policy design, while informing additional considerations, such as geological storage, social acceptance, environmental impact, and legal aspects (IEAGHG, 2021; Harzendorf et al., 2024; Gidden et al., 2025).

Several limitations should be noted. The analysis focuses on technical and weather-related cost drivers and does not incorporate regional variations in labor costs or financing conditions (Young et al., 2023; Egli et al., 2019). In practice, labor compensation in the energy and infrastructure sectors can differ by up to an order of magnitude across countries, potentially lowering DAC costs in lower-wages countries, particularly in parts of the Middle East and East Asia. Similarly, incorporating country-specific WACCs could shift cost competitiveness across regions, favoring lower-risk economies such as Australia, the United States, Canada, China, and Chile (Stargardt et al., 2025). Further, the analysis is limited to weather conditions, renewable energy availability and cost, and does not explicitly consider other key deployment constraints, including access to geological CO_2 storage, transport infrastructure, supply chain limitations, or deployment rate constraints, all of which influence the feasibility and spatial distribution of large-scale DAC deployment. Cost assumptions used in this study are based on literature-reported ranges and median projections for 2050, which implicitly reflect technology learning assumptions from the respective sources. These estimates carry inherent uncertainty due to both the long-time horizon of the cost estimates and methodological differences across studies. Among these, CAPEX exhibits the greatest variability and thus dominates overall cost uncertainty, making the relative cost competitiveness between L-DAC and S-DAC sensitive to the underlying assumptions. In addition, process model data for sorbent performance at sub-zero temperatures remain limited, constraining validation across cold climates. Assuming constant performance below 1 °C neglects potential reductions in mass transfer kinetics and may lead to an underestimation of capture costs in cold regions.

The regional spatial aggregation introduces limitations because averaging heterogeneous grid cells does not represent conditions at any single deployable site. For DAC, weather inputs are first averaged across intersecting grid cells and then used to evaluate performance, so nonlinear responses to temperature and humidity may cause the resulting estimates to over- or underestimate site-level performance by an amount not quantified in this study. For renewables, individual generation profiles are obtained at the grid-cell level and are then clustered into representative profiles for each technology, which preserve temporal variability but can still smooth local extremes. As a result, estimated energy storage requirements and energy costs may differ from those of a real project at a single site.

The DAC plant capacity factor is not fixed but emerges endogenously from the optimization, reflecting the cost-optimal operation of the plant under weather-dependent constraints. However, the model assumes unconstrained changes of plant operation between hourly time steps and does not account for ramping constraints or start-up and shut-down dynamics. This implies that DAC systems can adjust load instantaneously between hours. In practice, such flexibility might be limited, particularly for L-DAC, where components such as the electric calciner may require several hours to reach stable operating conditions (Shorey and Abdulla, 2024). As a result, frequent on/off cycling under fluctuating conditions may not be feasible. Neglecting these constraints could lead to an overestimation of operational flexibility and productivity, and an underestimation of the levelized cost and energy consumption. In addition, fixed operating conditions are assumed, and adaptive control strategies such as adjustments in airflow or solvent circulation rate, or regeneration conditions are not considered. These strategies could improve system performance under varying weather conditions. While sorbent replacement is included in operating costs, degradation effects or potential future improvements in sorbent performance are not explicitly modeled. Instead, these effects are represented in a simplified manner through literature-based cost assumptions. This may influence long-term productivity, operating costs, and overall cost estimates and should be considered when interpreting the results. Finally, this study reports the gross CO_2 removal, excluding upstream emissions from energy and materials. Although the emissions from DAC systems powered by renewable energy are expected to be close to zero, upstream life-cycle emissions associated with energy supply and system infrastructure are not considered in this study. Incorporating these effects would provide a more complete representation of net CO_2 removal, as outlined by Young et al. (Young et al., 2023) and should be considered in future work. More broadly, this work focuses on techno-economic parameters and does not explicitly consider socio-economic and policy-related factors, such as regional labor costs, financing conditions, or policy and regulatory frameworks, which may significantly influence the feasibility and spatial distribution of DAC deployment.

Future research can address several of these limitations. First, it would be valuable to incorporate the impacts of climate change, as DAC performance depends on weather conditions, and climate change may shift absolute productivity and costs by 2050. However, the overall regional ranking is likely to remain similar. Second, improved process models that capture real-world operating conditions, including dynamic operation and adaptive control strategies, would enhance the accuracy of cost estimates. Third, integrating DAC deployment with broader system constraints, such as CO_2 transport and storage infrastructure and policy frameworks, would provide a more comprehensive assessment of large-scale deployment. Addressing these aspects would enable a more robust and realistic evaluation of future DAC deployment.

AI declaration

Sections of this manuscript were revised to improve readability using OpenAI's ChatGPT. The authors reviewed and verified all AI-assisted content to ensure its accuracy and integrity.

CRediT authorship contribution statement

Kenneth Okosun: Writing – original draft, Visualization, Project administration, Methodology, Investigation, Formal analysis, Conceptualization. **Henrik Wenzel:** Writing – review & editing, Methodology. **Freia Harzendorf:** Supervision, Project administration, Funding acquisition, Conceptualization. **Thomas Schöb:** Writing – review & editing, Supervision, Project administration, Conceptualization. **Mak Đukan:** Writing – review & editing, Supervision, Conceptualization. **Jochen Linßen:** Project administration, Funding acquisition. **Detlef Stolten:** Project administration, Funding acquisition. **Jann M. Weinand:** Writing – review & editing.

Declaration of competing interest

The authors declare that they have no known competing financial interests or personal relationships that could have appeared to influence the work reported in this paper.

Acknowledgments

This work was performed as part of the project 'A Comprehensive Approach to Harnessing the Innovation Potential of Direct Air Capture and Storage for Reaching CO_2-Neutrality' (DACStorE), which is funded by the Initiative and Networking Fund of the Helmholtz Association (grant agreement number KA2-HSC-12). The Helmholtz Association further supported this research within the framework of the program "Energy System Design". The authors also greatly acknowledge the support of the NETs@Helmholtz Research School. Finally, the authors thank Darius Sultani (PIK Potsdam) for valuable discussions that helped shape the policy perspective of this work, particularly regarding the role of DAC in the context of Article 6 of the Paris Agreement and international carbon removal markets.

Supplementary materials

Supplementary material associated with this article can be found, in the online version, at doi:10.1016/j.ijggc.2026.104743.

Data availability

The techno-economic input data are available in the main text and the supplementary materials. The DAC performance time series, and the data underlying all figures are publicly available from the Zenodo repository: https://doi.org/10.5281/zenodo.21335047. These data and the corresponding results will also be made available through the DAC Atlas, an interactive graphical user interface developed within the DACStorE project: http://www.dac-atlas.com. All other input datasets are available from the sources cited in the manuscript.

References

An, K., Farooqui, A., McCoy, S.T., 2022. The impact of climate on solvent-based direct air capture systems. Appl. Energy 325, 119895. https://doi.org/10.1016/j.apenergy.2022.119895.

Beuttler, C., Charles, L., Wurzbacher, J., 2019. The role of direct air capture in mitigation of anthropogenic greenhouse gas emissions. Front. Clim. 1, 10. https://doi.org/10.3389/fclim.2019.00010.

Boerst, J., Pena Cabra, I., Sharma, S., Zaremsky, C., Iyengar, A.K.S, 2024. Strategic siting of direct air capture facilities in the United States. Energies. (Basel) 17 (15), 3755. https://doi.org/10.3390/en17153755. Jul 30.

Brooks, B.G.J., Geissler, C.H., An, K., McCoy, S.T., Middleton, R.S., Jd, O.-H., 2024. The performance of solvent-based direct air capture across geospatial and temporal climate regimes. Front. Clim. 6, 1394728. https://doi.org/10.3389/fclim.2024.1394728.

Cai, X., Coletti, M.A., Sholl, D.S., Mr, A.-D., 2024. Assessing impacts of atmospheric conditions on efficiency and siting of large-scale direct air capture facilities. JACS. Au. 4 (5), 1883–1891. https://doi.org/10.1021/jacsau.4c00082.

Caldera, U., Breyer, C., 2020. Strengthening the global water supply through a decarbonised global desalination sector and improved irrigation systems. Energy 200, 117507. https://doi.org/10.1016/j.energy.2020.117507.

C3S. ERA5 hourly data on single levels from 1940 to present. copernicus climate change service (C3S) climate data store (CDS); 2018. https://cds.climate.copernicus.eu/doi/10.24381/cds.adbb2d47.

Egli, F., Steffen, B., Schmidt, T.S., 2018. A dynamic analysis of financing conditions for renewable energy technologies. Nat. Energy 3 (12), 1084–1092. https://doi.org/10.1038/s41560-018-0277-y.

Egli, F., Steffen, B., Schmidt, T.S., 2019. Bias in energy system models with uniform cost of capital assumption. Nat. Commun. 10 (1), 4588. https://doi.org/10.1038/s41467-019-12468-z.

Elfving, J., Bajamundi, C., Kauppinen, J., Sainio, T., 2017. Modelling of equilibrium working capacity of PSA, TSA and TVSA processes for CO 2 adsorption under direct air capture conditions. J. CO2. Util. 22, 270–277. https://doi.org/10.1016/j.jcou.2017.10.010.

European Central Bank, 2024a. Euro foreign exchange reference rates.https://www.ecb.europa.eu/stats/policy_and_exchange_rates/euro_reference_exchange_rates/html/index.en.html.

European Central Bank, 2024b. Inflation and consumer prices. https://www.ecb.europa.eu/stats/macroeconomic_and_sectoral/hicp/html/index.en.html.

Fasihi, M., Efimova, O., Breyer, C., 2019. Techno-economic assessment of CO2 direct air capture plants. J. Clean. Prod. 224, 957–980. https://doi.org/10.1016/j.jclepro.2019.03.086.

Franzmann, D., Heinrichs, H., Stolten, D., 2025a. Global geothermal electricity potentials: a technical, economic, and thermal renewability assessment. Renew. Energy 250, 123199. https://doi.org/10.1016/j.renene.2025.123199.

Franzmann, D., Winkler, C., Dunkel, P., Stargardt, M., Burdack, A., Ishmam, S., et al., 2025b. Impact of Spatial Aggregation On Global Renewable Energy System With ETHOS.modelBuilder. SSRN. https://doi.org/10.2139/ssrn.5252316. https://www.ssrn.com/abstract=5252316.

Fuhrman, J., Clarens, A., Calvin, K., Doney, S.C., Edmonds, J.A., O'Rourke, P., et al., 2021. The role of direct air capture and negative emissions technologies in the shared socioeconomic pathways towards +1.5 °C and +2 °C futures. Environ. Res. Lett. 16 (11), 114012. https://doi.org/10.1088/1748-9326/ac2db0.

Fuss, S., Lamb, W.F., Callaghan, M.W., Hilaire, J., Creutzig, F., Amann, T., et al., 2018. Negative emissions—Part 2: costs, potentials and side effects. Environ. Res. Lett. 13 (6), 063002. https://doi.org/10.1088/1748-9326/aabf9f.

Gidden, M.J., Joshi, S., Armitage, J.J., Christ, A.B., Boettcher, M., Brutschin, E., et al., 2025. A prudent planetary limit for geologic carbon storage. Nature 645 (8079), 124–132. https://doi.org/10.1038/s41586-025-09423-y.

Hanna, R., Abdulla, A., Xu, Y., Victor, D.G., 2021. Emergency deployment of direct air capture as a response to the climate crisis. Nat. Commun. 12 (1). https://doi.org/10.1038/s41467-020-20437-0. Located at: Scopus.

Harzendorf, F., Markus, T., Ross, A., Valencia Cotera, R., Baust, C., Vögele, S., et al., 2024. Criteria for effective site selection of direct air capture and storage projects. Environ. Res. Lett. 19 (11), 111009. https://doi.org/10.1088/1748-9326/ad7a0f.

Holmes, G., Keith, D.W., 2012. An air–liquid contactor for large-scale capture of CO_2 from air. Philos. Trans. R Soc. Math. Phys. Eng. Sci. 370 (1974), 4380–4403. https://doi.org/10.1098/rsta.2012.0137.

IEA, 2022. Direct Air Capture: a key technology for net zero. International Energy Agency, Paris. https://www.iea.org/reports/direct-air-capture-2022.

IEA, 2024. Global Hydrogen Review 2024. International Energy Agency, Paris. https://www.iea.org/reports/global-hydrogen-review-2024.

IEA, 2025. ETP clean energy technology guide. International Energy Agency, Paris. https://www.iea.org/data-and-statistics/data-tools/etp-clean-energy-technology-guide?layout=list&selectedTechID=all.

IEAGHG, 2021. Global assessment of direct air capture costs. IEA Greenhouse Gas R&D Programme, UK. Report No. 2021-05. https://publications.ieaghg.org/technicalreports/2021-05%20Global%20Assessment%20of%20Direct%20Air%20Capture%20Costs.pdf.

IPCC, 2022. Climate Change 2022: Mitigation of Climate Change. Contribution of Working Group III to the Sixth Assessment Report of the Intergovernmental Panel on Climate Change. Cambridge University Press. https://doi.org/10.1017/9781009157926.

IRENA, 2022. Global Hydrogen Trade to Meet the 1.5 °C Climate goal: Part III – Green hydrogen Cost and Potential. International Renewable Energy Agency, Abu Dhabi. https://www.irena.org/-/media/Files/IRENA/Agency/Publication/2022/May/IRENA_Global_Hydrogen_Trade_Costs_2022.pdf.

Jacobs, G.K., Kerrick, D.M., Krupka, K.M., 1981. The high-temperature heat capacity of natural calcite (CaCO3). Phys. Chem. Miner. 7 (2), 55–59. https://doi.org/10.1007/BF00309451.

Jajjawi, A.S., Wenzel, H., Harzendorf, F., Weinand, J.M., Stolten, D., Peters, R., 2026. Weather-dependent direct air capture process modeling for techno-economic assessments. Energy Convers. Manage 351, 121003. https://doi.org/10.1016/j.enconman.2025.121003.

Keith, D.W., Holmes, G., St Angelo, D., Heidel, K., 2018. A process for capturing CO2 from the atmosphere. Joule 2 (8), 1573–1594. https://doi.org/10.1016/j.joule.2018.05.006.

Klütz, T., Knosala, K., Behrens, J., Maier, R., Hoffmann, M., Pflugradt, N., et al., 2025. ETHOS.FINE: a Framework for Integrated Energy System Assessment. J. Open. Source Softw. 10 (105), 6274. https://doi.org/10.21105/joss.06274.

Krull, L.F., Baum, C.M., Sovacool, B.K., 2025. A geographic analysis and techno-economic assessment of renewable heat sources for low-temperature direct air capture in Europe. Energy Convers. Manage 323, 119186. https://doi.org/10.1016/j.enconman.2024.119186.

Kucka, L., Kenig, E.Y., Górak, A., 2002. Kinetics of the gas−liquid reaction between carbon dioxide and hydroxide ions. Ind. Eng. Chem. Res. 41 (24), 5952–5957. https://doi.org/10.1021/ie020452f.

Küng, L., Aeschlimann, S., Charalambous, C., McIlwaine, F., Young, J., Shannon, N., et al., 2023. A roadmap for achieving scalable, safe, and low-cost direct air carbon capture and storage. Energy Environ. Sci. 16, 4280–4304. https://doi.org/10.1039/D3EE01008B.

McQueen, N., Desmond, M.J., Socolow, R.H., Psarras, P., Wilcox, J., 2021. Natural gas vs. Electricity for solvent-based direct air capture. Front. Clim. 2, 618644. https://doi.org/10.3389/fclim.2020.618644.

Pett-Ridge, J., Kuebbing, S., Mayer, A., Hovorka, S., Pilorgé, H., Ammar, H.Z., et al., 2023. Roads to removal: options for carbon dioxide removal in the United States. https://roads2removal.org/wp-content/uploads/07_RtR_Direct-Air-Capture.pdf.

Realmonte, G., Drouet, L., Gambhir, A., Glynn, J., Hawkes, A., Köberle, A.C., et al., 2019. An inter-model assessment of the role of direct air capture in deep mitigation pathways. Nat. Commun. 10 (1), 3277. https://doi.org/10.1038/s41467-019-10842-5.

Rickels, W., Proelß, A., Geden, O., Burhenne, J., Fridahl, M., 2021. Integrating carbon dioxide removal into European emissions trading. Front. Clim. 3, 690023. https://doi.org/10.3389/fclim.2021.690023.

Ryberg, D.S., 2019. Generation Lulls from the Future Potential of Wind and Solar Energy in Europe; 1st. RWTH Aachen University. https://doi.org/10.18154/RWTH-2020-10968. Dissertation. https://publications.rwth-aachen.de/record/805445.

Sendi, M., Bui, M., Mac Dowell, N., Fennell, P., 2022. Geospatial analysis of regional climate impacts to accelerate cost-efficient direct air capture deployment. One Earth. 5 (10), 1153–1164. https://doi.org/10.1016/j.oneear.2022.09.003.

Sendi, M., Bui, M., Mac Dowell, N., Fennell, P., 2024. Geospatial techno-economic and environmental assessment of different energy options for solid sorbent direct air capture. Cell Rep. Sustain. 1 (8), 100151. https://doi.org/10.1016/j.crsus.2024.100151.

Shorey, P., Abdulla, A., 2024. Liquid solvent direct air capture's cost and carbon dioxide removal vary with ambient environmental conditions. Commun. Earth. Environ. 5 (1), 607. https://doi.org/10.1038/s43247-024-01773-1.

Sievert, K., Schmidt, T.S., Steffen, B., 2024. Considering technology characteristics to project future costs of direct air capture. Joule 8, 979–999. https://doi.org/10.1016/j.joule.2024.02.005. Mar;S2542435124000606.

Smith, S.M., Geden, O., Gidden, M.J., Lamb, W.F., Nemet, G.F., Minx, J.C., et al., 2024. The State of carbon dioxide removal 2024, 2nd edition. Smith School of Enterprise and the Environment, University of Oxford. https://doi.org/10.17605/OSF.IO/F85QJ.

Sonntag, D., 1990. Important new values of the physical constants of 1986, vapour pressure formulations based on the ITS-90, and psychrometer formulae. https://api.semanticscholar.org/CorpusID:99374562.

Spreng, T.L., Danaci, D., Ram, P.D., Williams, D.R., Pini, R., Petit, C., 2026. Amine-appended hyper-crosslinked polymers for direct air capture of CO_2. ACS. Sustain. Chem. Eng. 14 (4), 1834–1846. https://doi.org/10.1021/acssuschemeng.5c08715.

Stargardt M., Hugenberg J., Winkler C., Heinrichs H., Linßen J., Stolten D. The striking impact of natural hazard risk on global green hydrogen cost. arXiv; 2025. doi:10.48550/ARXIV.2503.16009.

Steffen, B., Egli, F., Gumber, A., Đukan, M., Waidelich, P., 2025. A global dataset of the cost of capital for renewable energy projects. Sci. Data 12 (1), 1624. https://doi.org/10.1038/s41597-025-05912-x.

Terlouw, T., Pokras, D., Becattini, V., Mazzotti, M., 2024. Assessment of potential and techno-economic performance of solid Sorbent direct air capture with CO_2 storage in Europe. Environ. Sci. Technol. 58, 10567–10581. https://doi.org/10.1021/acs.est.3c10041.

UNFCCC, 2015. Article 6 of the Paris Agreement. United Nations Framework Convention on Climate Change.. In: https://unfccc.int/process-and-meetings/the-paris-agreement/article-6/article-62.

U.S. Energy Information Administration, 2025. International energy statistics: electricity consumption. U. S. Deparment of Energy. https://www.eia.gov/international/data/world/electricity/electricity-consumption/.

Van Der Spek, M., Bardow, A., Baum, C.M., Bolongaro, V., Dufour-Décieux, V., Esch, C., et al., 2025. An ecosystem of carbon dioxide removal reviews – part 1: direct air CO_2 capture and storage. Energy Environ. Sci. 18, 9713–9785. https://doi.org/10.1039/D5EE01732G.

Wei, Y.M., Peng, S., Kang, J.N., Liu, L.C., Zhang, Y., Yang, B., et al., 2025. Unlocking the economic potential of direct air capture technology: insights from a component-based learning curve. Technol. Forecast. Soc. Change 215, 124109. https://doi.org/10.1016/j.techfore.2025.124109.

Wenzel, H., Harzendorf, F., Okosun, K., Schöb, T., Weinand, J.M., Stolten, D., 2025. Weather conditions severely impact optimal direct air capture siting. Adv. Appl. Energy 19, 100229. https://doi.org/10.1016/j.adapen.2025.100229.

Wexler, A., 1976. Vapor pressure formulation for water in range 0 to 100 °C. A revision. J. Res. Natl. Bur. Stand. 80A.

Winkler, C., Dunkel, P., Chen, S., Belina, J., Heinrichs, H., Linßen, J., et al., 2025b. FZJ-IEK3-VSA/RESKit: v0.4.3. Zenodo. https://doi.org/10.5281/zenodo.17668776. https://zenodo.org/doi/10.5281/zenodo.17668776.

Winkler, C., Heinrichs, H., Ishmam, S., Bayat, B., Lahnaoui, A., Agbo, S., et al., 2025a. Participatory mapping of local green hydrogen cost-potentials in Sub-Saharan Africa. Int. J. Hydrog. Energy 112, 289–321. https://doi.org/10.1016/j.ijhydene.2025.02.015.

Young, J., McQueen, N., Charalambous, C., Foteinis, S., Hawrot, O., Ojeda, M., et al., 2023. The cost of direct air capture and storage can be reduced via strategic deployment but is unlikely to fall below stated cost targets. One Earth. 6 (7), 899–917. https://doi.org/10.1016/j.oneear.2023.06.004.